J Pharmacol Sci **107**, 370 – 379 (2008)

Journal of Pharmacological Sciences
©2008 The Japanese Pharmacological Society

Full Paper

Reactive Oxygen Species Mediate Oridonin-Induced HepG2 Apoptosis Through p53, MAPK, and Mitochondrial Signaling Pathways

Jian Huang[1,2], Lijun Wu[1], Shin-ichi Tashiro[3], Satoshi Onodera[3], and Takashi Ikejima[2,*]

[1]*Department of Phytochemistry,* [2]*China-Japan Research Institute of Medical and Pharmaceutical Sciences, Shenyang Pharmaceutical University, 103 Wenhua Road, Shenyang, 110016, P.R. China*
[3]*Department of Clinical and Biomedical Science, Showa Pharmeceutical University, Tokyo 194-8543, Japan*

Received February 20, 2008; Accepted June 4, 2008

Abstract. Oridonin, a diterpenoid isolated from *Rabdosia rubescences*, could induce apoptosis through the generation of reactive oxygen species (ROS) in human hepatoma HepG2 cells. p53, a specific inhibitor of pifithrin α (PFT α), markedly inhibited ROS generation and apoptosis, showing that p53 was responsible for the cytotoxity of oridonin through mediation by ROS. Moreover, the ROS activated the p38 kinase, which in turn promoted the activation of p53, as verified by evidence showing that the ROS scavenger *N*-acetyl-cysteine (NAC) not only blocked the phosphorylation of p38 but also partially inhibited the activation of p53, and the p38 inhibitor SB203580 reduced the activation of p53 as well. Mitochondria were either the sources or the targets of ROS. This study showed that oridonin stimulated mitochondrial transmembrane permeabilization in a ROS-dependent manner because NAC almost thoroughly reversed the drop of mitochondrial transmembrane potential ($\Delta\psi$m) and the release of cytochrome *c* from the mitochondrial inter-membrane space into cytosol. Furthermore, as a result of mitochondrial permeability transition, procaspases-9 and -3 were cleaved into 37- and 17-kDa proteolytic products, respectively, which acted as executors of oridonin-induced apoptosis.

Keywords: oridonin, reactive oxygen species (ROS), p53, p38, mitochondria

Introduction

Basic cancer research has produced remarkable advances in our understanding of cancer biology and cancer genetics. Among the most important of these advances is the realization that apoptosis and its related regulative genes have a profound effect on the malignant phenotype (1). Until now, apoptosis induction by various cytotoxic anticancer agents has almost been one of the most effective methods for cancer therapy. Morphologic characteristics of apoptosis include cell membrane bebbling, cell shrinkage, chromatin condensation, and nucleosomal fragmentation and formation of membrane-bound apoptotic bodies (2 – 5). Apoptosis is a process in which cell death is initiated and completed in an orderly manner through activation and/or synthesis of gene products necessary for cell destruction. Among these gene products, p53, mitogen-activated protein kinase (MAPK) family, Bcl-2 family, and cysteine-dependent aspartate-specific proteases (caspase) family play important roles in regulating the apoptotic process (6 – 9).

Reactive oxygen species (ROS), including hydroxyl radicals, superoxide anions, singlet oxygen, and hydrogen peroxide, are generated as by-products of cellular metabolism (10, 11). Organisms have developed their own antioxidant mechanisms including low-molecular-weight antioxidant molecules, such as glutathiones (GSH); melatonin; and various antioxidant enzymes including superoxide dismutase (SOD), catalase (CAT), glutathione peroxidase (GSH-Px), and glutathione reductase. These enzyme activities are higher in the liver than in other tissues (12). Oxidative stress indicates an imbalance state between production of ROS and antioxidant defenses. If oxidative stress persists, oxidative damage to critical biomolecules accumulates and eventually results in several biological effects such as alterations in signal transduction and gene expression for mitogenesis, mutagenesis, and cell death (13). Consis-

*Corresponding author. ikejimat@vip.sina.com
Published online in J-STAGE
doi: 10.1254/jphs.08044FP

tent with the reports, many studies also suggest that ROS are important mediators of apoptosis (14 – 16). Therefore, we investigated the role of ROS in the induction of apoptosis in human liver cell lines.

Rabdosia rubescens, a herbal medicine, has been traditionally used in China for curing carcinoma of the digestive tract. Oridonin is a diterpenoid isolated from *R. rubeseens* and has been reported to have various pharmacological and physiological effects such as anti-inflammation, anti-bacteria, and anti-tumor effects (17 – 19). With regard to its anti-tumor activity, some reports have demonstrated that oridonin exhibits remarkable inhibitory effects on breast carcinoma, non-small cell lung cancers, acute promyelocytic leukemia, and glioblastoma multiforme; and some reports have also showed that oridonin has cytotoxic effects on various cancers such as human melanoma A375-S2, human cervical carcinoma HeLa, human breast adenocarcinoma MCF-7, and murine fibrosarcoma L929 (20 – 24). During our research on the anti-tumor effect of oridonin, we found that it gave rise to a great deal of ROS in human hepatoma cells HepG2, and the cells underwent apoptosis consequently. So in this study, we investigated the roles of ROS in oridonin-induced HepG2 cell apoptosis.

Materials and Methods

Reagents

Oridonin (Lot: 111721-200501) was obtained from the Beijing Institute of Biological Products (Beijing, China). The chemical structure of oridonin was assigned by comparing the chemical and spectral data (^{1}H-NMR, ^{13}C-NMR) with those reported in the literature. The purity of the oridonin was measured by HPLC [Column: 4.6 mm × 250 mm, type: CAPCELL PAK C18 ACR (Shiseido, Tokyo); solvent phase: methanol:H_2O, 55:45] and determined to be 97.4%. Oridonin was dissolved in dimethyl sulfoxide (DMSO) to make a stock solution. The DMSO concentration was kept below 0.05% in all the cell cultures and did not exert any detectable effect on cell growth or cell death.

Fetal calf serum (FCS) was from the Dalian Biological Reagent Factory (Dalian, China). RPMI 1640 medium was from Gibco/BRL (Gaithersburg, MD, USA). *N*-Acetyl-cysteine (NAC), Hoechst 33258, rhodamine-123, 3-(4,5-dimethylthiazol-2-yl)-2,5-diphenyltetrazolium bromide (MTT), 3,3-diaminobenzidine tetrahydrochloride (DAB), and 2',7'-dichlorofluorescein diacetate (DCF-DA) were purchased from Sigma Chemical (St. Louis, MO, USA). The p53 inhibitor pifithrin α (PFT α) was from Biomol International (Plymouth Meeting, PA, USA). The ERK inhibitor PD98059, p38 inhibitor SB203580, JNK inhibitor SP600125, and antibodies against caspase-9 and -3 were obtained from Calbiochem (La Jolla, CA, USA). Antibodies against cytochrome *c* (Cyto. *c*), p53, phospho-p53 (Ser 392), p38, phospho-p38 (Tyr 182), β-actin, and horseradish peroxidase (HRP)-conjugated secondary antibodies (goat-anti-rabbit and goat-anti-mouse) were purchased from Santa Cruz Biotechnology (Santa Cruz, CA, USA). TACS^{TM}2 TDT-DAB *In Situ* Apoptosis Detection Kit was obtained from Trevigen (Gaithersburg, MD, USA).

Cell culture

The human hepatoma cells HepG2 were purchased from American Type Culture Collection (#HB-8065; ATCC, Manassas, VA, USA). The cells were cultured in RPMI-1640 medium supplemented with 10% FCS and 0.03% L-glutamine (Gibco), and maintained at 37°C with 5% CO_2 in a humidified atmosphere.

Cytotoxity assay

HepG2 cells were incubated in 96-well plates (NUNC, Roskilde, Denmark) at a density of 1×10^5 cells per well. The cells were pretreated with NAC, PFT α, PD98059, SB203580, and SP600125 at the given concentrations for 1 h and then incubated with oridonin for different time periods. Four hours before the end of incubation, 20 μl MTT solution (5.0 mg/l) was added to each well. The crystals were dissolved in 100 μl DMSO. Absorbance was measured with an ELISA reader (TECAN SPECTRA; Wetzlar, Germany). The cytotoxic effect was expressed as the relative percentage of cell death, which was calculated as follows:

$$\text{Cell death (\%)} = [A_{570}\text{ (control)} - A_{570}\text{ (compound)}] / [A_{570}\text{ (control)} - A_{570}\text{ (blank)}] \times 100$$

Observation of morphological changes

HepG2 cells were divided into two groups, seeded into culture plates, and cultured overnight. One group was cultured in the RPMI-1640 as the medium control. The other was treated with 30 μM oridonin and cultured for 24 h. The cellular morphology was observed using phase contrast microscopy (Olympus, Tokyo).

The HepG2 cells were cultured as above and treated with oridonin for 24 h. Apoptotic nuclear morphology was also assessed using Hoechst 33258. Cells were fixed with 3.7% paraformaldelyde at room temperature for 30 min, and then they were washed and stained with 167 μM Hoechst 33258 at 37°C for 30 min. The cells were washed and resuspended in phosphate-buffered saline (PBS) for morphologic observation by fluorescence microscopy (Leica, Wetzlar, Germany).

Terminal deoxynucleotidyl transferase-mediated Dutp nick end-labeling (TUNEL) assay

The TUNEL assay was used for detection of DNA strand breaks. The detection was carried out according to the instructions of the TACS^{TM}2 TDT-DAB *In Situ* Apoptosis Detection Kit. Briefly, the cells were rinsed once with PBS and fixed in 3.7% buffered formaldehyde at room temperature for 10 min. The fixed cells were pretreated with 10% H_2O_2, and end-labeling was performed with TdT labeling reaction mix at 37°C for 1 h. Nuclei exhibiting DNA fragmentation were visualized by incubation in 3',3-diamino benzidine (Sigma) for 7 min. The cells were counter-stained with methyl green and observed under light microscopy. The nuclei of apoptotic cells were stained dark brown and TUNEL-positive HepG2 cells were determined with relative percentage by randomly counting 100 cells.

Measurement of intracellular ROS generation

After treatment with 30 μM oridonin for the indicated time periods, the cells were incubated with 10 mM DCF-DA at 37°C for 15 min. The intracellular ROS mediated oxidation of DCF-DA to the fluorescent compound 2',7'-dichlorofluorescein (DCF). Then cells were harvested and the pellets were suspended in 1 ml PBS. Samples were analyzed at an excitation wave length of 480 nm and an emission wave length of 525 nm by FACScan flowcytometry (Becton Dickinson, Franklin Lakes, NJ, USA).

Preparation of mitochondrial and cytosolic extracts

The tested cell groups were collected by centrifugation at 200 × *g* at 4°C for 5 min and then washed twice with ice-cold PBS. The cell pellets were resuspended in ice-cold homogenizing buffer, including 250 mM sucrose, 20 mM HEPES, 10 mM KCl, 1 mM EDTA, 1 mM EGTA, 1.5 mM $MgCl_2$, 1 mM DTT, 1 mM PMSF, 1 μg/ml aprotinin, and 1 μg/ml leupeptin. After homogenization (40 strokes), the homogenates were centrifuged at 4,200 × *g* at 4°C for 30 min. The supernatant was used as the cytosol fraction and the pellet was resolved in lysis buffer, including 50 mM Hepes (pH 7.4), 1% Triton-X 100, 2 mM sodium orthovanadate, 100 mM sodium fluoride, 1 mM edetic acid, 1 mM PMSF, 10 mg/l aprotinin (Sigma), and 10 mg/l leupeptin (Sigma) as the membrane fraction.

Observation of mitochondria membrane potential

Mitochondria membrane potential was observed by the fluorescent dye rhodamine-123. After incubation with 30 μM oridonin for the indicated time periods, the cells were stained with 1 mg/ml rhodamine-123 and incubated at 37°C for 15 min. The fluorescence intensity of cells *in situ* was observed under fluorescence microscopy (Olympus).

Western blot analysis

HepG2 cells were cultured for different time periods, both adherent and floating cells were collected, and then Western blot analysis was performed. Briefly, the cell pellets were resuspended in lysis buffer consisting of 50 mM Hepes (pH 7.4), 1% Triton-X 100, 2 mM sodium orthovanadate, 100 mM sodium fluoride 1 mM edetic acid, 1 mM PMSF, 10 mg/l aprotinin, and 10 mg/l leupeptin and lysed at 4°C for 60 min. After 13,000 × *g* centrifugation for 15 min, the protein content of the supernatant was determined by a protein assay reagent (Bio-Rad, Hercules, CA, USA). The protein lysates were separated by electrophoresis in 12% SDS polyacrylamide gel and transferred to a nitrocellulose membrane. The membrane was blocked with 5% skim milk and then incubated with the indicated primary antibodies against p53, phospho-p53, p38, phospho-p38, cytochrome *c*, caspase-9, and caspase-3. After that, the membrane was incubated with secondary antibodies, goat anti-rabbit and goat anti-mouse IgG conjugated with peroxidase (HRP) (Santa Cruz Biotechnology), and visualized by using DAB as the HRP substrate.

Statistical analysis of the data

All results were confirmed in at least three separate experiments. The data are expressed as means ± S.D. Statistical comparisons were made by Student's *t*-test. $P<0.05$ was considered significant.

Results

Cytotoxic effects of oridonin against HepG2 cells

To detect the cytotoxic effects of oridonin on the

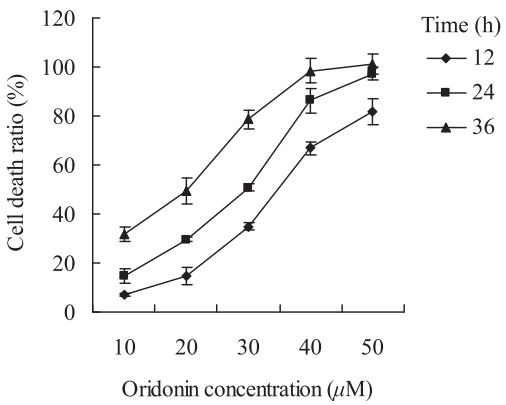

Fig. 1. The cytotixity of oridonin against HepG2 cells. The cells were treated with various doses of oridonin for 12, 24, or 36 h. Cell death ratio was measured by MTT assay. n = 3, mean ± S.D.

HepG2 cells, the cells were cultured with 10 – 50 μM oridonin for 12, 24, and 36 h. Oridonin induced cell death in a dose- and time-dependent manner. Treatment of HepG2 cells with 30 μM oridonin for 24 h resulted in approximately 50% cell death (Fig. 1).

Oridonin induces apoptotic cell death in HepG2 cells

To determine whether HepG2 cells treated with oridonin underwent apoptosis, TUNEL assay was carried out. HepG2 cells were cultured with 0, 10, 20, 30, 40, and 50 μM oridonin for 24 h; and the ratio of TUNEL-positive cells was 2.3 ± 1.5%, 11.7 ± 1.5%,

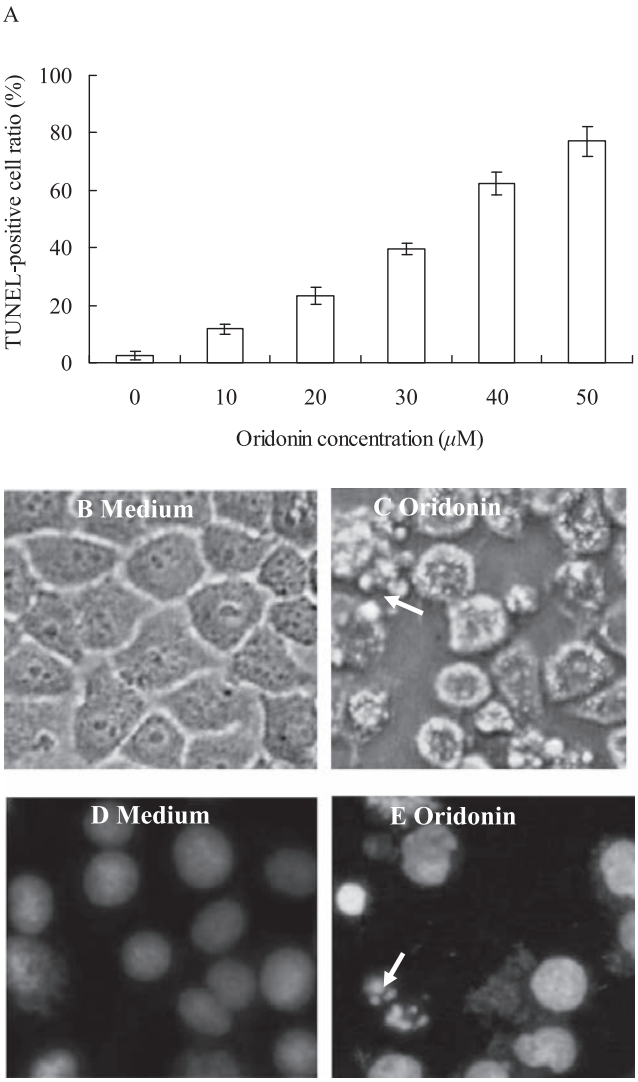

Fig. 2. Oridonin induced apoptotic cell death in HepG2 cells. A: The cells were treated with 0, 10, 20, 30, 40, or 50 μM oridonin for 24 h. The TUNEL assay was carried out for detection of apoptotic cells. n = 3, mean ± S.D. B – E: The cells were treated with 30 μM oridonin for 24 h, and cellular morphologic changes were observed by means of phase contrast microscopy (B, C: ×400 magnification) or Hoechst 33258 (D, E: ×400 magnification) staining.

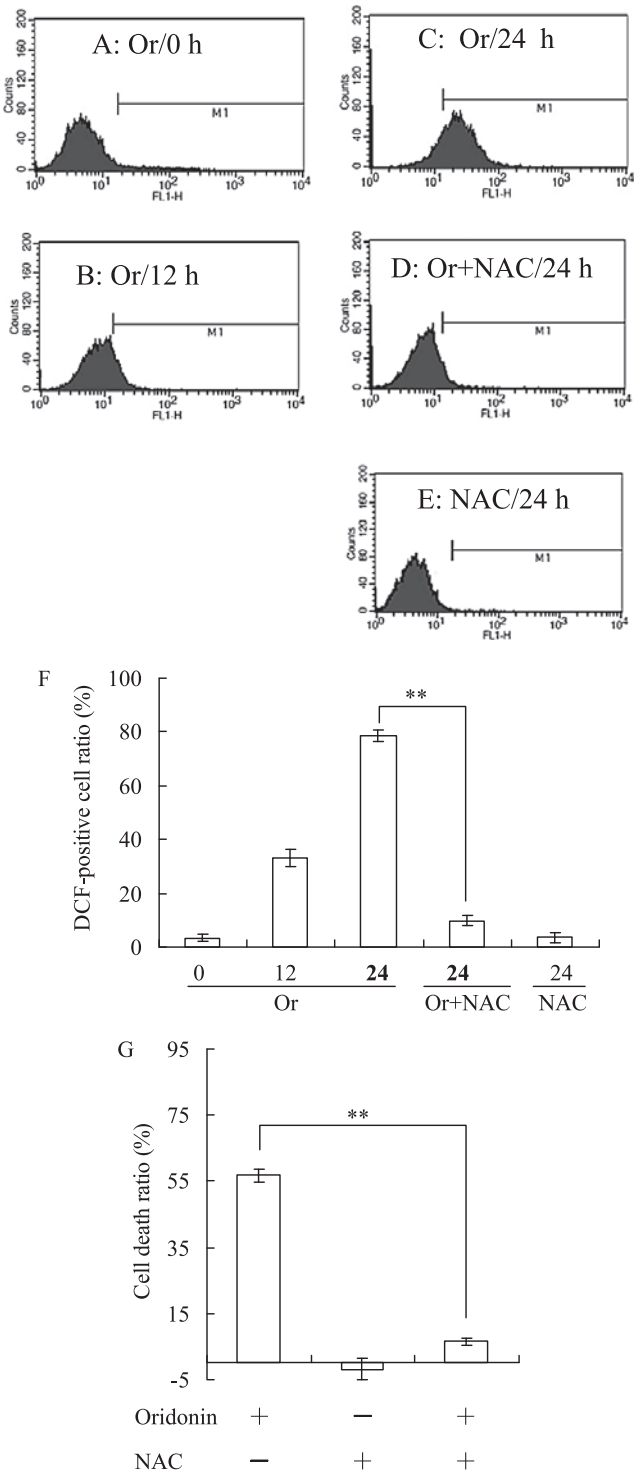

Fig. 3. Oridonin stimulated the generation of ROS that mediated HepG2 apoptosis. A – E: The cells were cultured with 30 μM oridonin (Or) for 0 (A), 12 (B), and 24 (C, D) h in the absence or presence of 1 mM NAC (D, E). F: The generation of ROS was measured by using the ROS-detecting fluorescent dye DCF-DA in FACScan flowcytometry. The corresponding linear diagram of FACScan flowcytometry is shown. n = 3, mean ± S.D. $^{**}P<0.01$. G: The cells were pretreated with or without 1 mM NAC for 1 h and then treated with 30 μM oridonin for 24 h. Cell death ratio was measured by MTT assay. n = 3, mean ± S.D. $^{**}P<0.01$.

23.3 ± 3.1%, 39.7 ± 2.1%, 62.3 ± 4.2%, and 77.2 ± 5.3%, respectively (Fig. 2A).

To further confirm the result that oridonin induced HepG2 apoptotic cell death, we examined the morphologic changes. When HepG2 cells were cultured with oridonin at 30 μM for 24 h, apoptotic changes were observed as compared with the medium control group. Oridonin-treated HepG2 cells underwent contraction and showed membrane blebbing and granular apoptotic bodies, but the cells in the medium control group did not show these apoptotic changes (Fig. 2: B and C). The apoptotic changes were further confirmed by Hoechst 33258 staining of cell nuclei. In the control group, nuclei of HepG2 cells were round and homogeneously stained, but 30-μM oridonin–treated cells showed marked nuclear fragmentation and granular apoptotic bodies (Fig. 2: D and E).

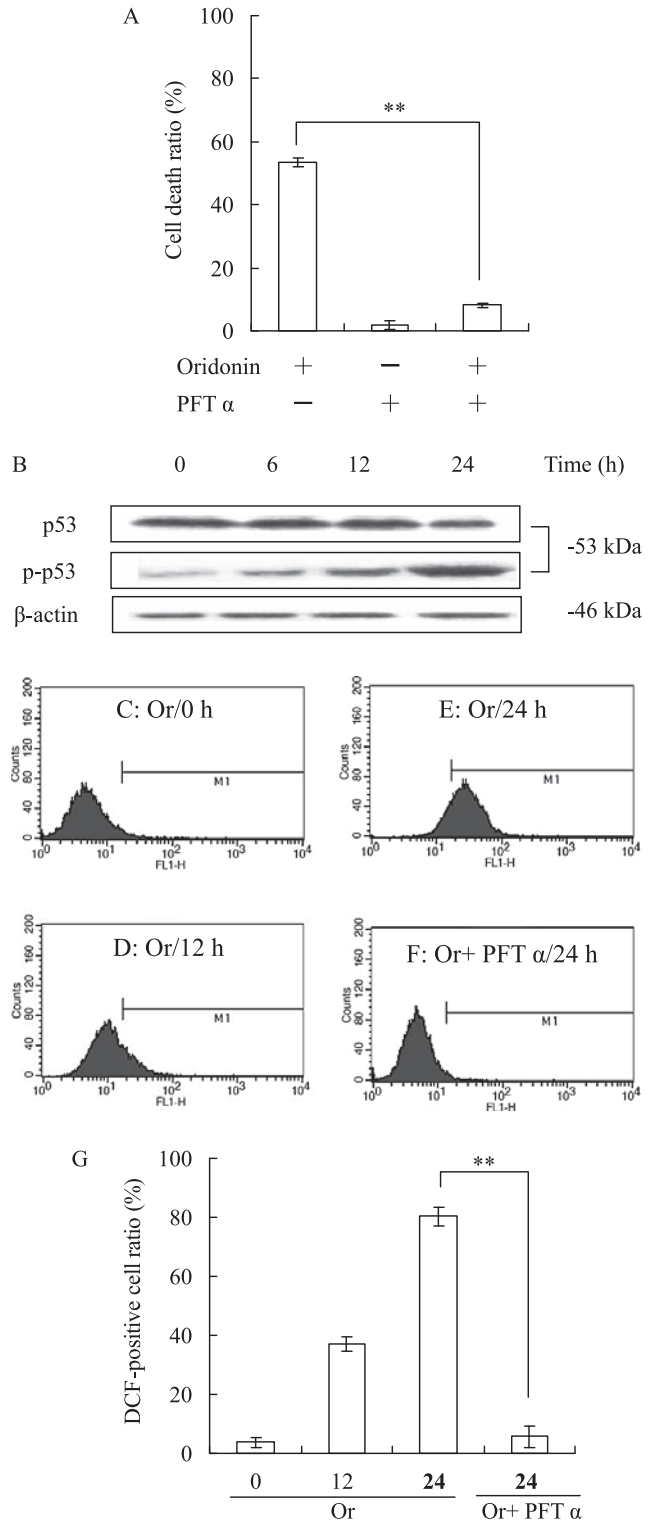

Fig. 4. p53 mediated ROS generation in oridonin-induced HepG2 apoptosis. A: The cells were pretreated with15 μM PFT α for 1 h and then cultured with 30 μM oridonin for 24 h. Cell death ratio was measured by MTT assay. n = 3, mean ± S.D. ***P*<0.01. B: The cells were treated 30 μM oridonin for 0, 6, 12, or 24 h; and cell lysates were separated by 12% SDS-PAGE electrophoresis, and p53 and phospho-p53 protein expression was detected by Western blot analysis. C – F: The cells were cultured with 30 μM oridonin (Or) for 0 (C), 12 (D), and 24 (E, F) h in the absence or presence of 15 μM PFT α (F). G: The generation of ROS was measured by using the ROS-detecting fluorescent dye DCF-DA in combination with FACScan flowcytometry. The corresponding linear diagram of FACScan flowcytometry is shown. n = 3, mean ± S.D. ***P*<0.01.

Oridonin triggered ROS generation which mediated HepG2 apoptosis

ROS are considered to play an important role in apoptosis in various types of cells (14 – 16). To investigate whether oridonin stimulated ROS generation in HepG2 cells, we measured intracellular ROS level by using the ROS-detecting fluorescence dye DCF-DA, and the generation of ROS was evidenced by the increased intensity of DCF fluorescence. After HepG2 cells were exposed to 30 μM oridonin for the indicated time periods, moderate generation of ROS were observed at 12 h and the level of ROS increased significantly at 24 h. The ratio of DCF-positive cells was 2.32, 33.24, and 78.57% at 0, 12, and 24 h, respectively (Fig. 3: A, B, and C). As expected, the ROS scavenger NAC at 1 mM markedly decreased the level of ROS from 78.57% to 9.86% at 24 h (Fig. 3: D and F).

It has been reported that ROS may play a dual role in apoptosis. On the one hand, ROS may function as initiators of apoptosis, but on the other hand, ROS have also anti-apoptotic effects, especially in inflammatory cells (25). To further confirm that ROS acted as initiators in oridonin-induced HepG2 apoptosis, the cells were co-incubated with 1 mM NAC in the presence of 30 μM oridonin for 24 h and NAC almost completely inhibited the oridonin-induced apoptosis from 56.7% to 6.6% (Fig. 3G). All these results indicated that ROS mediated apoptosis in oridonin-treated HepG2 cells.

p53 was involved in oridonin-induced HepG2 apoptosis through mediating ROS generation

The tumor suppressor gene product p53 has been reported to mediate apoptosis in many experimental systems, which is responsible for its tumor suppressive function (26). In our study, the p53-specific inhibitor PFT α was applied to evaluate the function of p53 in oridonin-induced HepG2 apoptosis. After incubation of HepG2 cells with 30 μM oridonin for 24 h, 15 μM PFT α significantly reduced apoptosis from 52.5% to 8.1% (Fig. 4A). To further confirm this result, Western blot analysis was carried out to detect the p53 and phospho-p53 expressions. After treatment of HepG2 cells with 30 μM oridonin for different time periods, the expression of p53 did not change, but the level of phospho-p53 markedly increased at 6 h (Fig. 4B).

Recent studies have indicated that p53 causes apoptosis through a multi-step process and ROS are sometimes downstream mediators of p53-dependent apoptosis (27, 28). Therefore, we examined the effect of p53 on the generation of ROS triggered by oridonin. When HepG2 cells were treated with 30 μM oridonin for 24 h in the presence of 15 μM PFT α, PFT α obviously lowered the level of ROS from 80.39% to 5.61% (Fig. 4: E, F, and G), indicating that p53 participated in oridonin-induced apoptosis through the generation of ROS.

ROS contributes to further activation of p53 through activation of p38 kinase in oridonin-treated HepG2 cells

The MAPK family members including extracellular signal-regulated protein kinase (ERK), c-Jun N-terminal kinase (JNK), and p38 play important roles in regulation of apoptosis. The ERK pathway is predominantly activated by mitogens through a Ras-dependent mechanism and it is required for cell proliferation and differentiation, but JNK and p38 are activated by pro-inflammatory cytokines and various environmental stresses (29). In our study, the functions of MAPK in oridonin-induced HepG2 apoptosis were examined by using specific inhibitors for p38 (SB203580), JNK (SP600125), and ERK (PD98059). After incubation of HepG2 cells with 30 μM oridonin for 24 h, 10 μM SP600125 and 10 μM PD98059 did not influence the cytotoxity of oridonin (Fig. 5A). In contrast, 10 μM of the p38 inhibitor SB203580 partially inhibited the cell death from 55.6% to 25.1% (Fig. 5A). On the basis of these results and in combination with the report that ROS could lead to activation of p38 in TRAIL/Apo2L-induced apoptosis (30), the effect of ROS on the activation of p38 was investigated by means of Western blot analysis. After treatment of HepG2 cells with 30 μM oridonin for different time periods, the level of phospho-p38 began to increase at 12 h. However, in the presence of 1 mM NAC or 10 μM SB203580, SB203580 and NAC almost thoroughly reversed the phosphorylation of p38 (Fig. 5B), indicating that the activation of p38 was dependent on ROS in oridonin-induced HepG2 apoptosis.

Recently, it has been reported that p38 kinase directly phosphorylates N-terminal serine residues of p53, which in turn activate the p53 signaling pathway (31 – 33). According to these studies, Western blot analysis was performed to examine the effects of NAC and SB203580 on the level of phospho-p53. As shown in Fig. 5C, when HepG2 cells were treated with oridonin for 6, 12, and 24 h, the enhanced phospho-p53 expression at 24 h was significantly reduced by 1 mM NAC or 10 μM SB203580 (Fig. 5C). All these results suggested that ROS contributed to further activation of p53 through activation of p38 kinase.

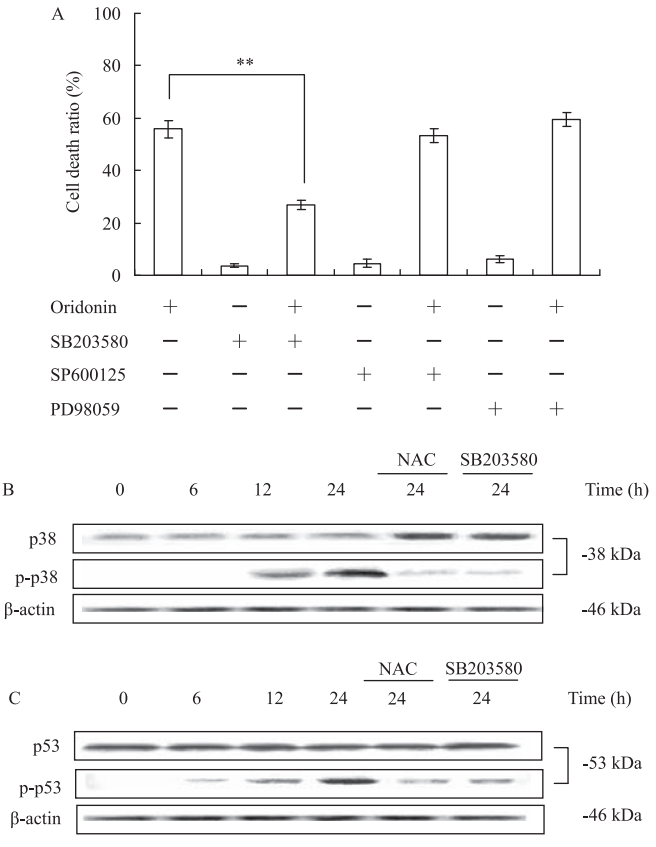

Fig. 5. ROS activated the p38, which further promoted the phosphorylation of p53. A: The cells were pretreated with 10 μM SB203580, 10 μM SP600125, or 10 μM PD98059 for 1 h and then cultured with 30 μM oridonin for 24 h. Cell death ratio was measured by MTT assay. n = 3, mean ± S.D. $^{**}P<0.01$. B and C: The cells were treated 30 μM oridonin for 0, 6, 12, or 24 h in the absence or presence of 1 mM NAC or 10 μM SB203580; and cell lysates were separated by 12% SDS-PAGE electrophoresis, and p38, phospho-p38 (B) and p53, phospho-p53 (C) protein expressions were detected by Western blot analysis. n = 3, mean ± S.D.

ROS decrease the mitochondrial transmembrane potential (Δψm) and mediated the oridonin-induced HepG2 apoptosis through mitochondrial signaling pathway

Mitochondria are deeply involved in the regulation of cell death and the mitochondrial membrane permeabilization pore has been shown to be sensitive to the redox state, and ROS can also induce mitochondrial membrane permeabilization both in vitro and in vivo (34, 35). When mitochondria membrane is permeabilized, cytochrome *c*, which is normally confined in the mitochondrial intermembrane space, is found in the cytosol of cells undergoing apoptosis (36, 37). Cytochrome *c* release is frequently coincident with a disruption of the mitochondrial transmembrane potential (*Δψ*m), which has been defined as an early stage of apoptosis (34, 35). Based on these results, we evaluated whether ROS targeted the mitochondria and thereby decreases the *Δψ*m in oridonin-treated HepG2 cells. The integrity of mitochondrial membranes of the cells was examined by rhodamine-123 staining and the decrease in rhodamine-123 fluorescence intensity reflected the loss of *Δψ*m. The fluorescence intensity of oridonin-treated cells for the indicated time periods was observed under a fluorescence microscope. The cells incubated with 30 μM oridonin showed a weaker green fluorescence at 24 h (Fig. 6C), compared with the bright green fluorescence in the medium-cultured cell group (Fig. 6A). In the case of the NAC-co-treated group, the NAC rescued the loss of *Δψ*m, as verified by the enhanced intensity of fluorescence at 24 h (Fig. 6D).

When cytochrome *c* is released from mitochondria, it forms a complex with Apaf-1 and procaspase-9, resulting in activation of caspase-9, which then processes and activates other caspases, such as caspase-3, to carry out the biochemical execution of apoptosis (38). In order to further confirm that the mitochondrial signaling pathway was initiated by ROS, the expressions of cytochrome *c*, caspase-9, and caspase-3 in HepG2 cells treated with 30 μM oridonin in the absence or presence of NAC were examined by Western blot analysis. The results showed that the level of cytochrome *c* in mitochondria began to decrease at 12 h, which was consistent with the increase of cytochrome *c* in cytosol. However, the release of cytochrome *c* from mitochondria into cytosol was suppressed by NAC (Fig. 6E). With the cytochrome *c* released, the caspases-9 and -3 were activated, as proved by the appearance of 37- and 17-kDa proteolytic products at 18 h (Fig. 6F). These results indicated that ROS caused the *Δψ*m loss, cytochrome *c* release, and caspases activation, which accounted for the oridonin-induced HepG2 apoptosis.

Taken together, all these results demonstrated that in oridonin-induced HepG2 apoptosis, p53 mediated the generation of ROS, which activated p38 kinase, and the activated p38 further stimulated the activation of p53. In

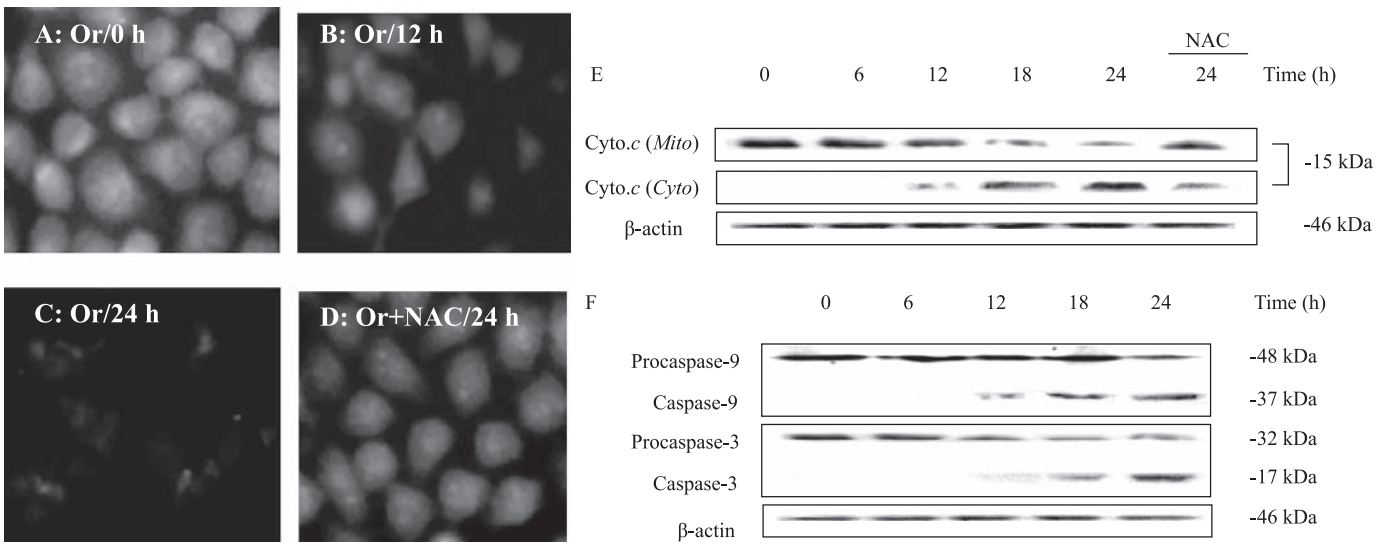

Fig. 6. ROS caused a decrease in the *Δψ*m, so that cytochrome *c* was released into cytoplasm and subsequently caspase-9 and -3 were activated in HepG2 cells incubated with oridonin. The cells were incubated with 30 μM oridonin (Or) for 0 (A), 12 (B), 24 (C) h, or coincubated with 30 μM oridonin and 1 mM NAC for 24 h (D); then the cells were loaded with a membrane-sensitive probe, 1 mg/ml rhodamine-123, for 30 min and observed using fluorescence microscopy. The cells were treated 30 μM oridonin for 0, 6, 12, 18, or 24 h in the absence or presence of 1 mM NAC. The cell lysates were separated by 12% SDS-PAGE electrophoresis; and protein expressions of cytochrome *c* (Cyto. *c*) (E), both in the cytoplasm (*Cyto*) and the mitochondria (*Mito*), and caspase-9 and -3 (F) were detected by Western blot analysis.

addition, ROS targeted the mitochondria and caused decrease of $\Delta\psi$ms. As a consequence, the HepG2 cells underwent apoptosis via the cytochrome *c*/caspase-9 and -3 signaling pathway.

Discussion

This study demonstrated that oridonin was able to induce apoptosis in human hepatoma HepG2 cells through the generation of ROS. It was generally believed that oxidative stress was an important regulator of the apoptosis in certain cell types (39). Also, many studies suggested that exposure to ROS induced apoptosis in a variety of cell types by inducing endonuclease activation and subsequent DNA damage (40, 41). Another important regulator of apoptosis was p53, and p53 protein was a tumor suppressor that transmits signals arising from various forms of cellular stress including DNA damage and hypoxia to genes and factors (42). It had also been reported that p53 protein caused apoptosis, using ROS as downstream mediators (27, 28). In our study, Western blot analysis and MTT assay showed that p53 was activated and transmitted apoptotic signals in oridonin-treated HepG2 cells. The p53 signaling pathway was divided into two parts, upstream and downstream of p53; and the downstream components of the p53 pathway are p53 transcriptional targets. It was reported that more than half of those genes were directly or indirectly involved in metabolism of ROS, and ROS were required in the p53-dependent apoptotic pathway (43). The results obtained from this study showed that the p53 inhibitor PFT α markedly blocked the generation of ROS, implying that ROS was induced in a p53-dependent pathway in oridonin-treated HepG2 cells.

p38, one of the members of MAPK family, had been implicated in regulation of various cellular processes (29). A number of studies indicated that activation of p38 played a crucial role in apoptosis induced by various stimuli, such as ceramide and nerve growth factor depletion (44, 45). Activation of p38 kinase has also been implicated in anticancer drug–induced apoptosis (29). In our study, pretreatment of SB203580 was effective in preventing oridonin-induced apoptosis, indicating that p38 was involved in this process. Lee and his colleagues had shown that p38 was responsive to ROS and participated in apoptosis, for example, nitric oxide stimulated the phosphorylation of p38 in HL-60 cells and H_2O_2 induced the activation of p38 in vascular cells (30). It was also reported that the activation of p38 induced by TRAIL/Apo2L was effectively inhibited by pretreatment of GSH and estrogen, indicating that ROS were activated upstream of p38 (30). In this study, oridonin promoted the activation of p38, and the ROS scavenger NAC effectively blocked the phosphorylation of p38, demonstrating that p38 was activated through a ROS-dependent process in oridonin-treated HepG2 cells. Reports showed that expression of oncogenic Ras resulted in activation of p38, which in turn led to activation of p53 (46). In addition, p38 kinase could activate the p53 signaling pathway through direct phosphorylation of N-terminal serine residues of p53 (31 – 33). In oridonin-treated HepG2 cells, the activation of p38 by ROS further contributed to the activation of p53, which was further verified by the evidence that the high level of phospho-p53 was effectively inhibited by SB203580 and NAC, respectively. All these results suggested that p53 mediated the generation of ROS, which accounted for p38 activation, and the activated p38 contributed to further p53 activation; thus a positive feedback loop arose in oridonin-treated HepG2 cells.

Mitochondria showed signs of outer membrane and/or inner membrane permeabilization when exposed to a variety of pro-apoptotic stimulus (36). For example, TGF β-mediated ROS production in fetal hepatocytes provoked the loss of $\Delta\psi$m and the release of cytochrome *c* (47). Also, reducing superoxide levels could inhibit the loss of $\Delta\psi$m in the activated T cell, and high levels of ROS could lead to megamitochondria formation in a model of hepatocyte cell death (48, 49). Indeed, some reports also showed that ROS either acted as activators of mitochondrial permeability transition or a consequence of this transition, depending on the death stimulus (50). Here, the results of rhodamine-123 staining to detect the $\Delta\psi$m showed that oridonin-induced ROS production in HepG2 cells preceded the loss of $\Delta\psi$m, as confirmed by the evidence that ROS scavenger NAC effectively blocked the drop of $\Delta\psi$m. In mitochondria, when membrane permeabilization occurred, cytochrome *c* was releasd from the mitochondrial intermembrane space into the cytosol, and then caspases-9 and -3 were activated (38). In this study, incubation of HepG2 cells with oridonin for 12 h made reduced the expression of cytochrome *c* in mitochondria, accompanied by the high level of cytochrome *c* in cytosol; and this process was correspondingly suppressed by NAC. Consistent with this result, caspases-9 and -3 were cleaved into a 37- and 17-kDa fragment, respectively, at 18 h. These results indicated that ROS was responsible for mitochondria transmembrane permeabilization, thereby causing the release of cytochrome *c* and the activation of caspases-9 and -3, which executed the oridonin-induced HepG2 apoptosis.

In summary, oridonin induced HepG2 apoptosis in a time- and dose-dependent manner through the mediation of ROS. To investigate the mechanism, we found that p53 was responsible for the generation of ROS, which

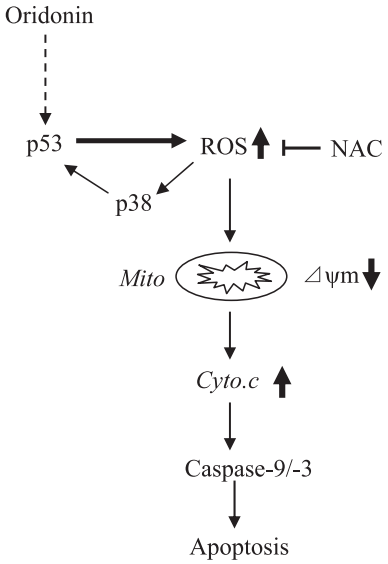

Fig. 7. Summary of the proposed mechanism for the apoptosis induced by oridonin in HepG2 cells. Oridonin would indirectly activate p53 that mediated the generation of ROS. The ROS would contribute to the loss of $\Delta\psi$m, the release of cytochrome *c* (*Cyto. c*) from the mitochondria (*Mito*), and the activation of caspase-9/-3. In addition, ROS further promoted the activation of p53 through activation of p38 kinase, forming a positive feedback loop.

led to the activation of p38 kinase; and the activated p38 in turn promoted the activation of p53, forming a positive feedback loop. Furthermore, ROS decreased the $\Delta\psi$m and provoked the release of cytochrome *c*. Consequently, caspases-9 and -3 were activated and executed the oridonin-induced HepG2 cell apoptosis (Fig. 7).

References

1 Lowe SW, Lin AW. Apoptosis in cancer. Carcinogenesis. 2000;21:485–495.

2 Kim SO, Han J. Pan-caspase inhibitor zVAD enhances cell death in RAW 246.7 macrophages. J Endotoxin Res. 2001;7:292–296.

3 Kawazoe N, Watabe M, Masuda Y, Nakajo S, Nakaya K. Tiamil is involved in the regulation of bufalin-induced apoptosis in human leukemia cells. Oncogene. 1999;18:2413–2421.

4 Hill PA, Tumber A, Meikle MC. Multiple extracellular signals promote osteoblast survival and apoptosis. Endocrinology. 1997;138:3849–3858.

5 Mizukami S, Kikuchi K, Higuchi T, Urano Y, Mashima T, Tsuruo T, et al. Imaging of caspase-3 activation in HeLa cells stimulated with etoposide using a novel fluorescent probe. FEBS Lett. 1999;453:356–360.

6 Banin S, Moyal L, Shieh S, Taya Y, Anderson CW, Chessa L, et al. Enhanced phosphorylation of p53 by ATM in response to DNA damage. Science. 1998;281:1674–1677.

7 Petrache I, Choi ME, Otterbein LE, Chin BY, Mantell LL, Horowitz S, et al. Mitogen-activated protein kinase pathway mediates hyperoxia-induced apoptosis in cultured macrophage cells. Am J Physiol. 1999;277:L589–L595.

8 Green DR, Reed JC. Mitochondria and apoptosis. Science. 1998;281:1309–1312.

9 Enari M, Sakahira H, Yokoyama H, Okawa K, Iwamatsu A, Nagata S. A caspase-activated DNase that degrades DNA during apoptosis and its inhibitor ICAD. Nature. 1998;391:43–50.

10 Klamt F, Dal-Pizzol F, Conte da Frota MLJR, Walz R, Andrades ME, da Silva EG, et al. Imbalance of antioxidant defense in mice lacking cellular prion protein. Free Radic Biol Med. 2001; 30:1137–1144.

11 Crack PJ, Taylor JM. Reactive oxygen species and the modulation of stroke. Free Radic Biol Med. 2005;38:1433–1444.

12 Yuan GJ, Ma JC, Gong ZJ, Sun XM, Zheng SH, Li X. Modulation of liver oxidant-antioxidant system by ischemic preconditioning during ischemia/reperfusion injury in rats. World J Gastroenterol. 2005;11:1825–1828.

13 Ermak G, Davies KJ. Calcium and oxidative stress: from cell signaling to cell death. Mol Immunol. 2002;38:713–721.

14 Su CC, Lin JG, Li TM, Chung JG, Yang JS, Ip SW, et al. Curcumin-induced apoptosis of human colon cancer colo 205 cells through the production of ROS, Ca^{2+} and the activation of caspase-3. Anticancer Res. 2006;26:4379–4389.

15 Simbula G, Columbano A, Ledda-Columbano GM, Sanna L, Deidda M, Diana A, et al. Increased ROS generation and p53 activation in alpha-lipoic acid-induced apoptosis of hepatoma cells. Apoptosis. 2007;12:113–123.

16 Reinecke F, Levanets O, Olivier Y, Louw R, Semete B, Grobler A, et al. Metallothionein isoform 2A expression is inducible and protects against ROS-mediated cell death in rotenone-treated HeLa cells. Biochem J. 2006;395:405–415.

17 Osawa K, Yasuda H, Maruyama T, Morita H, Takeya K, Itokawa H. Antibacterial trichorabdal diterpenes from Rabdosia Trichocarpa. Phytochemistry. 1994;36:1287–1291.

18 Fuji K, Node M, Sai M, Fujita E, Takeda S, Unemi N. Terpenoids LIII. Antitumor activity of trichorabdals and related compounds. Chem Pharm Bull. 1989;37:1472–1476.

19 Fujita T, Takeda Y, Sun HD, Minami Y, Marunaka T, Takeda S, et al. Cytotoxic and antitumor activities of Rabdosia diterpenoids. Planta Med. 1988;54:414–417.

20 Liu YQ, You S, Tashiro S, Onodera S, Ikejima T. Activation of phosphoinositide, protein kinase C, and extracellular signal-regulated kinase is required for oridonin-enhanced phagocytosis of apoptotic bodies in human macrophage-like U937 cells. J Pharmcol Sci. 2005;98:361–371.

21 Zhang CL, Wu LJ, Zuo HJ, Tashiro S, Onodera S, Ikejima T. Cytochrome *c* release from oridonin-treated apoptotic A375-S2 cells is dependent on p53 and extracellular signal-regulated kinase activation. J Pharmcol Sci. 2004;96:155–163.

22 Ikezoe T, Chen SS, Tong XJ, Heber D, Taguchi H, Koeffler HP. Oridonin induces growth inhibition and apoptosis of a variety of human cancer cells. Int J Oncol. 2003;23:1187–1193.

23 Marks LS, Dipaola RS, Nelson P, Chen S, Heber D, Belldegrum AS, et al. PC-SPES: herbal formulation for prostate cancer. Urology. 2002;60:369–377.

24 Zhang CL, Wu LJ, Tashiro S, Onodera S, Ikejima T. Oridonin induced A375-S2 cell apoptosis via bax-regulation caspase pathway activation, dependent on the cytochrom *c*/caspase-9 apoptosome. J Asia Natl Prod Res. 2004;6:127–138.

25 Simon HU, Haj-Yehia A, Levi-Schaffer F. Role of reactive oxygen species (ROS) in apoptosis induction. Apoptosis. 2000;

5:415–418.
26 Bunz F, Dutriaux A, Lengauer C, Waldman T, Zhou S, Brown JP, et al. Requirement for p53 and p21 to sustain G2 arrest after DNA damage. Science. 1998;282:1497–1501.
27 Polyak K, Xia Y, Zweier JL, Kinzler KW, Vogelstein B. A model for p53-inducible apoptosis. Nature. 1997;389:300–305.
28 Johnson TM, Yu ZX, Ferrans VJ, Lowenstein RA, Finkel T. Reactive oxygen species are downstream mediators of p53-dependent apoptosis. Proc Natl Acad Sci U S A. 1996;93:11848–11852.
29 Schaeffer HJ, Weber MJ. Mitogen-Activated Protein Kinases: Specific Messages from Ubiquitous Messengers. Mol Cell Biol. 1999;19:2435–2444.
30 Lee MW, Park SC, Yang YG, Yim SO, Chae HS, Bach JH, et al. The involvement of reactive oxygen species (ROS) and p38 mitogen activated protein (MAP) kinase in TRAIL/Apo2L-induced apoptosis. FEBS Lett. 2002;512:313–318.
31 Bulavin DV, Saito S, Hollander MC, Sakaguchi K, Anderson CW, Appella E, et al. Phosphorylation of human p53 by p38 kinase coordinates N-terminal phosphorylation and apoptosis in response to UV radiation. EMBO J. 1999;18:6845–6854.
32 Huang C, Ma WY, Maxiner A, Sun Y, Dong Z. p38 kinase mediates UV-induced phosphorylation of p53 protein at serine 389. J Biol Chem. 1999;274:12229–12235.
33 Kim SJ, Hwang SG, Shin DY, Kang SS, Chun JS. p38 kinase regulates nitric oxide-induced apoptosis of articular chondrocytes by accumulating p53 via NFkappa B-dependent transcription and stabilization by serine 15 phosphorylation. J Biol Chem. 2002;277:33501–33508.
34 Green DR, Reed JC. Mitochondria and apoptosis. Science. 1998;281:1309–1312.
35 Kroemer G, Reed JC. Mitochondrial control of cell death. Nature Med. 2000;6:513–519.
36 Yang J, Liu X, Bhalla K, Kim CN, Ibrado AM, Cai J, et al. Prevention of apoptosis by Bcl-2: release of cytochrome *c* from mitochondria blocked. Science. 1997;275:1129–1132.
37 Kluck RM, Bossy-Wetzel E, Green DR, Newmeyer DD. The release of cytochrome *c* from mitochondria: a primary site for Bcl-2 regulation of apoptosis. Science. 1997;275:1132–1136.
38 Li P, Nijhawan D, Budihardjo I, Srinivasula SM, Ahmad M, Alnemri ES, et al. Cytochrome *c* and dATP-dependent formation of Apaf-1/caspase-9 complex initiates an apoptotic protease cascade. Cell. 1997;91:479–489.
39 Jabs T. Reactive oxygen intermediates as mediators of programmed cell death in plants and animals. Biochem Pharmacol. 1999;57:231–245.
40 Buttke TM, Sandstrom PA. Oxidative stress as a mcdiator of apoptosis. Immunol Today. 1994;15:7–10.
41 Ueda N, Shah SV. Endonuclease-induced DNA damage and cell death in oxidant injury to renal tubular epithelial cells. J Clin Invest. 1992;90:2593–2597.
42 Prives C. Signaling to p53: breaking the MDM2 – p53 circuit. Cell. 1998;95:5–8.
43 Polyak K, Xia Y, Zweier JL, Kinzler KW, Vogelstein B. A model for p53-induced apoptosis. Nature. 1997;389:300–305.
44 Brenner B, Koppenhoefer U, Weinstock C, Linderkamp O, Lang F, Gulbins E. Fas- or Ceramide-induced apoptosis is mediated by a Racl-regulated activation of Jun N-terminal kinase/p38 kinases and GADD153. J Biol Chem. 1997;272:22173–22181.
45 Xia Z, Dickens M, Raingeaud J, Davis RJ, Greenberg ME. Opposing effects of ERK and JNK-p38 MAP kinases on apoptosis. Science. 1995;270:1326–1331.
46 Wang W, Chen JX, Liao R, Deng Q, Zhou JJ, Huang S, et al. Sequential activation of the MEK-extracellular signal-regulated kinase and MKK3/6-p38 mitogen-activated protein kinase pathways mediates oncogenic ras-induced premature senescence. Mol Cell Biol. 2002;22:3389–3403.
47 Rodrigues CM, Ma X, Linehan-Stieers C, Fan G, Kren BT, Steer CJ. Ursodeoxycholic acid prevents cytochrome *c* release in apoptosis by inhibiting mitochondrial membrane depolarization and channel formation. Cell Death Differ. 1999;6:842–854.
48 Hildeman DA, Mitchell T, Teague TK, Henson P, Day BJ, Kappler J, et al. Reactive oxygen species regulate activation-induced T cell apoptosis. Immunity. 1999;10:735–744.
49 Karbowski M, Kurono C, Wozniak M, Ostrowski M, Teranishi M, Nishizawa Y, et al. Free radical-induced megamitochondria formation and apoptosis. Free Radic Biol Med. 1999;26:396–409.
50 Green DR, Reed JC. Mitochondria and apoptosis. Science. 1998;281:1309–1312.